

# ALUMINIUM HONEYCOMB UNDER QUASI-STATIC COMPRESSIVE LOADING: AN EXPERIMENTAL INVESTIGATION

Mohamad Radzai Said and Chee-Fai Tan\*

Received: Feb 27, 2008; Revised: Dec 22, 2008; Accepted: Dec 23, 2008

## Abstract

The effect of the aluminium honeycomb with the crushing load-displacement characteristics and the mode of deformation under quasi-loading were investigated. The experimental results for aluminium honeycomb under quasi-static condition applied in 3 principal directions are reported. The specimens under lateral loading showed three zones: Zone 1 is the initial elastic state, and then followed by the plateau region in zone 2. Zone 3 shows a monotonically stiffening region, associated with densification of the material. However, under axial compression, initial collapse occurs at a peak load, and is then followed by the amplitudes of little peaks, which signify progressive folding collapse. The collapse load due to lateral loading is compared with mean load in axial compression loading.

**Keywords:** Aluminium, honeycomb, quasi-static compressive loading

## Introduction

The use of aluminium honeycomb in the sandwich structure continues to increase rapidly due to the wide field of application, for example aircraft, wind energy systems, ships and automobiles. The sandwich composites are made from multi-layered materials with high strength skins and low density core material. Lateral and axial crushing of cellular solids has received a great deal of attention, in the context of energy absorption (Reid and Peng, 1997; Gibson and Ashby, 1998). Reid *et al.* (1993) and Reid and Peng (1997) have recently reviewed the literature on the crushing of wood under dynamic loading conditions and have provided formulae

for the crushing stress versus displacement for wood. Many aspects of the behaviour of cellular solids are summarized well in the book by Gibson and Ashby. There is a great interest in the current and potential use of these materials for packaging, as impact energy absorbers and their use as core material in lightweight sandwich structures. Gibson and Ashby devote a chapter of their book to the selection of material for low speed impact application. Honeycomb, in particular, has been used as a protective material for high velocity impact and is often used as an impact energy absorbing material. This paper presents the results of the study in which speci-

---

*Designed Intelligence Group, Department of Industrial Design Technical University Eindhoven P.O. Box 513, 5600MB Eindhoven, Netherland. E-mail: c.f.tan@tue.nl*

\* *Corresponding author*

mens of aluminium honeycomb were subjected to axial and lateral compression under quasi-static conditions.

Pioneering investigations on the plastic crushing of honeycombs under axial compressive loads were reported from the California Institute of Technology by McFarland (1963, 1964). He developed a semi-empirical formulae of the mean crushing stress for honeycomb under axial compression, which depends on the ratio of thickness and side length,  $t/b$ . He concluded that, for  $t/b$  ratios  $\leq 0.07$ , a shear failure mode is the one that essentially produces a gross progressive collapse. The mechanics of deformation were seen to be unchanged under impact loads. Even though his model is not totally compatible with the experimentally observed collapse modes and his approach is of a semi-empirical nature, he provided a great thrust into the research of hexagonal honeycombs.

Wierzbicki (1983) has provided an improved model for the crushing of honeycombs. By incorporating both bending and extension in the deformation mechanism, he produced an expression of the mean crushing stress,  $(\sigma_{cr}^*)_m$  for regular hexagons and honeycombs in which two of six sides of a cell have double thickness due to forming process. He obtained the expressions by minimising the mean crushing stress with reference to half wavelength of plastic folds,  $H$ . Wu and Jiang (1997) have performed tests on aluminium honeycombs under axial compression and compared the results with theoretical predictions. However, they wrongly quoted that  $H$  depends on the wall thickness,  $t$  and minor diameter,  $s$ .

The response of honeycombs under lateral compression has been studied by Gibson *et al.* (1982), Klinworth and Stronge (1988, 1999) and others. However, Gibson *et al.* first derived the expressions for the linear-elastic modulus and for the elastic and plastic collapse stresses for honeycombs under lateral loading. They assumed beam theory analysis for elastic regions and large deformation theories for plastic regions. The elastic analysis only includes the

bending action of the walls of the cells. Masters and Evans (1996) included the effect of bending and stretching mechanism. This leads to the conclusion that the collapse stress can be related to cell-wall properties (elastic modulus Young,  $E_s$  and yield stress,  $\sigma_{ys}$ ), the cell shapes (cell wall angle,  $\theta$  and the ratio of cell face length to cell side length,  $h/l$ ) and the ratio of thickness to cell side length,  $t/l$ . More recent studies are due to Triantafyllidis and Schraad (1998) and Papka and Kyriakides (1994). Papka and Kyriakides have carried out experiments and performed computer simulations in their studies on the response of hexagonal aluminium honeycombs (Al-5052-H39) subjected to quasi-static loading across corners. They have used ABAQUS Finite Element Analysis in their numerical studies and compared the results with their experiments. However, they have not studied the simulated responses of honeycombs compressed across faces. In the most recent paper, Said and Reddy (2001) have simulated the honeycomb compressed across faces as well as in axial direction.

In this paper, the experimental data on aluminium honeycomb under quasi-static compressive loading is presented. The main body of this work is concerned with the crushing load-displacement characteristics and the mode of deformation of honeycomb under quasi-static loading in 3 principal directions from elastic to plastic collapse.

## Experimental Developments

Cubic specimens of side length 100 or 80 mm made of aluminium honeycomb manufactured by CIBA-GEIGY (AL3003-H19) were used. This honeycomb had an overall density of  $83 \text{ kg/m}^3$ . The cells of the honeycomb supplied by the manufacturer were slightly irregular hexagons (Figure 1(a) and 1(b)) with face length,  $h$  of 3.1 mm, side length,  $l$  of 4.38 mm and wall thickness;  $t$  was 0.0635 mm, as shown in Figure 1(c). The properties of the material (aluminium alloy) as specified by manufacturer are Modulus of elasticity,  $E = 69 \text{ MPa}$ , Yield stress,  $\sigma_y = 165 \text{ MPa}$ , Poisson's ratio,  $\nu = 0.33$  and ultimate

tensile strength,  $\sigma_{ult} = 200$  MPa. The 100 mm-cube specimens (Figure 1(a)) consisted of 255 cells with 15 rows and 17 columns. The 80 mm-cube (Figure 1(b)) had 168 cells, 12 rows by 14 columns. The specimens were carefully prepared so that the edges of the cross sections were clean.

The honeycomb samples were compressed between two rigid platens in each of the three principal directions: lateral compression across faces, lateral compression across corners and compression along the direction of cell axis. The load-displacement traces obtained from the displacement controlled at 10 mm/min.

## Experimental Results

The load-displacement traces and the deforming mode are presented below.

### Lateral Compression of Honeycombs Across Faces

Typical load-displacement traces for three specimens (100 mm-cube) shown in Figure 2 indicate good repeatability. The deformation can be divided into three zones. Zone 1 is the initial,

stiff, elastic state, which is followed by an elastic-plastic state that terminates with collapse signified by a zero slope of the load-displacement curve. Zone 2 is the plateau region where sequential crushing of lines of cells takes place at a nearly constant load, with very small, non-uniform load fluctuations. Finally, zone 3 starts with the termination of plateau (zone 2) and shows a monotonically stiffening region, associated with densification of the material. A sequence of deformed pictures of a typical specimen showing the mode of deformation corresponding to displacement identified by points (0), (1), (2), (3), (4), and (5) as per Figure 2. Figure 3 shows a sequence photograph of the deformation of aluminium honeycomb specimen compressed across faces.

During compression of the honeycomb in zone 1, the deformation of all cells was symmetric about their axes and uniform through the length of the specimen. A slight barreling of the specimen was also observed. At collapse load 0.28 kN (a deflection of about 14 mm), a line of cells inclined to the loading axis (at about  $60^\circ$ ) began to deform in an unstable manner causing

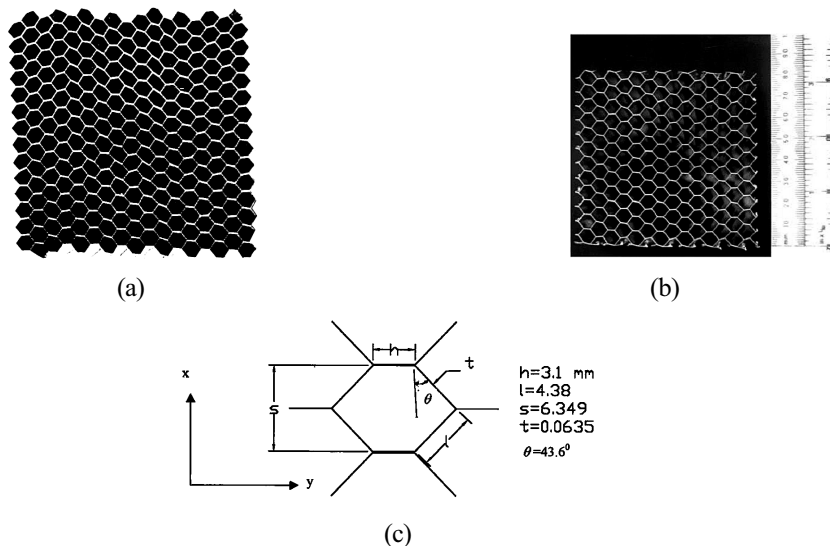


**Figure 1. An undeformed aluminium honeycomb with irregular hexagonal cell**

- (a) 100 mm  $\times$  100 mm  $\times$  100 mm, with 15 rows and 17 columns
- (b) 80 mm  $\times$  80 mm  $\times$  80 mm, with 12 rows and 14 columns
- (c) Dimension of hexagonal cells (in mm)

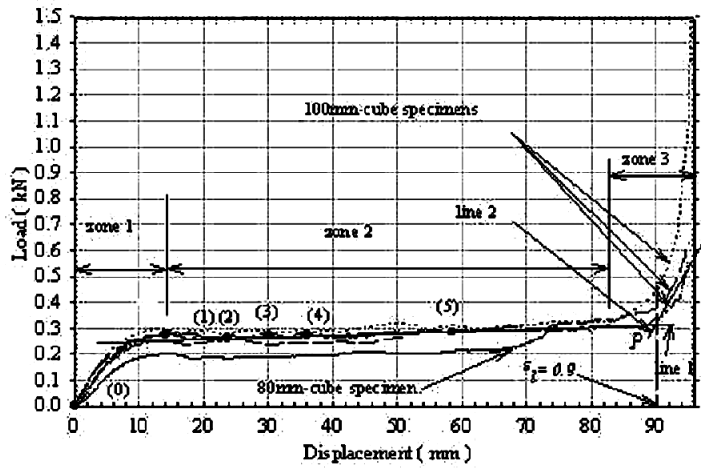


Figure 2. The load-displacement curves of honeycomb laterally compressed across faces for three 100 mm cube specimens showing repeatability results, and a 80mm cube specimen

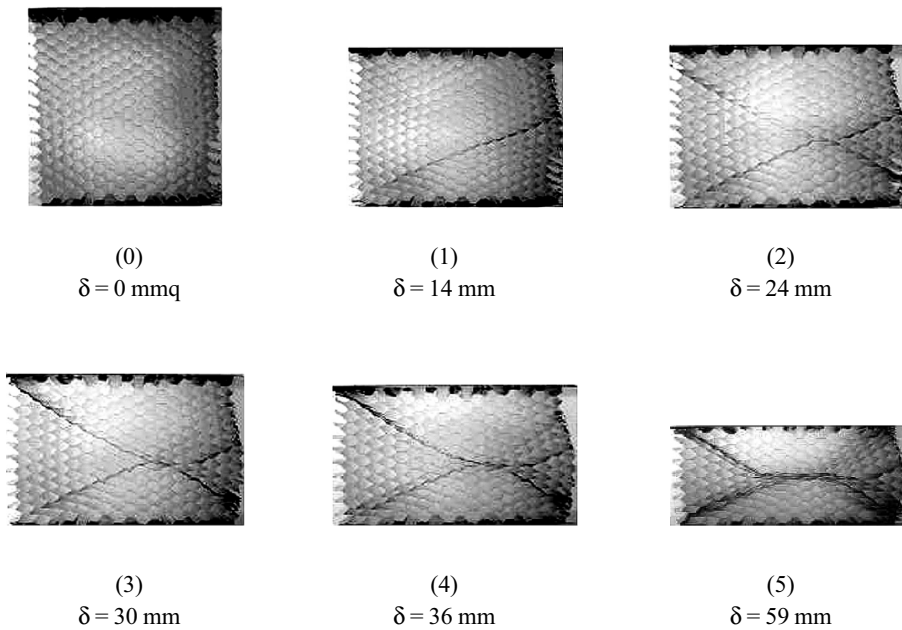


Figure 3. A sequence of photographs showing the deformation of aluminium honeycomb specimen compressed across faces

localisation of deformation. The result of the onset of this localisation is clearly seen as a shear band in the deforming specimen shown in Figure 3, corresponding to point (1) in Figure 2. The shear band was initially at about  $30^\circ$  to the platens' face edge. The load dropped slightly and gradually after the initiation of the shear band (at a displacement of 14 mm) signifying plastic collapse until this line of cells was completely crushed. From then on, the load remained fairly steady. Another shear band starting from the opposite end of first line was seen just after point (1). This was at about  $35^\circ$  to the platens' face edge. The deforming specimen, which indicates 2 shear bands (at  $\delta = 24$  mm), is shown in Figure 2 corresponding to point (2) in Figure 3. As the displacement increased, deformation spread to the lines of cells adjacent to the initial shear bands while the remaining cells were largely undeformed. The spreading of deformation can be seen in Figure 3 at displacements of 30 mm, 36 mm, and 59 mm, which relate to points (3), (4) and (5) as per Figure 2.

When almost all cells were closed, the load started to increase very rapidly. This is the densification stage (zone 3) of deformation in the honeycomb. This zone is not useful for energy absorption, as the strain does not increase appreciably. This limiting value of strain is the so called locking strain,  $\epsilon_l$ . Different definitions

can be found for the locking strain. Here, locking strain is defined by the intersection of two lines. Line 1 is the plateau and line 2 is parallel to the initial elastic line and at a tangent to the stress-strain curve in the stiffening region. For example, point  $P$  in Figure 2 is a locking strain in the curve, which shows 0.9.

### Lateral Compression of Honeycombs Across Corners

A 100 mm-cube and 80 mm-cube honeycomb specimens is used in the lateral compression experiment. Figure 4 shows a typical load-displacement curve and a corresponding sequence of deformations is shown in Figure 5. The load-displacement curve is similar to that for a specimen crushed across faces in the first and third zones. There is a difference in the second zone in that the load increases gradually in the present case. Zone 2 starts with a small reduction of load followed by the collapse load, as the localization occurred in the middle region of the specimen. As the reduction of the load continued, about half line of the cells in the central row of the specimen were seen to have collapsed in shear as seen in Figure 5 at point (1) (a deflection of 17 mm). This shear deformation spread to the whole row and then to the neighbouring rows of cells. Figure 5 shows the specimen compressed at displacement of 34 mm

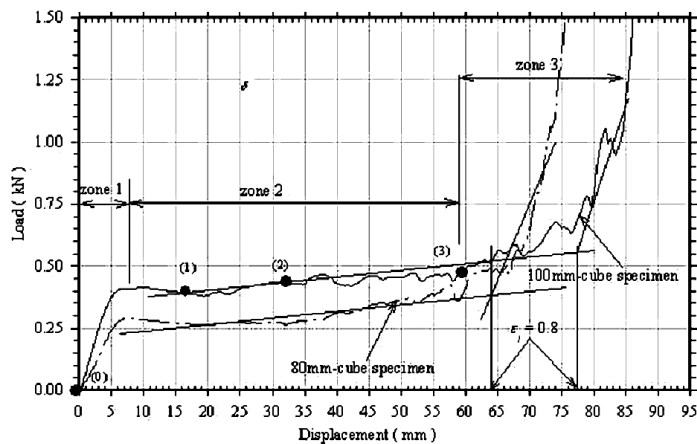


Figure 4. Typical load-displacement curves of laterally compressed (across corners) 100 mm-cube and 80 mm-cube honeycomb specimens

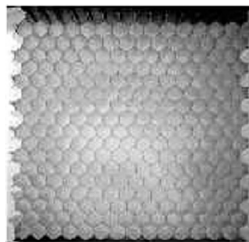
(point (2)), three rows in the middle of specimen are completely crushed. Each collapsed row is associated with the small fluctuations in the load-displacement characteristics. At the 60 mm compression (point (3)), when almost all cells of the bottom half of the specimen have collapsed (Figure 5) the load started to increase. This monotonically steep gradient of the load-deflection curve indicates the end of zone 2. The locking strain is found at about 0.8. The collapse load of honeycombs compressed across corners is higher by about 50% compared with loading across faces. This may be due to the double thickness of the cell wall in line with the loading direction.

### Axial Compression of Honeycombs

In the axial compression of honeycomb, a 80 mm-cube and 100 mm-cube specimen are used. Figure 6 shows typical load-displacement curves for honeycombs under axial compression for 80 mm-cube and 100 mm-cube specimens. Two curves are given in each case to show the repeatability. The curves for each specimen show elastic, perfectly plastic, and locking type characteristics. A sharp reduction of load separates the elastic and plastic regions.

Initial collapse occurs at a load, which is about twice of the average steady load causing progressive crushing. The amplitudes of the little peaks, which signify progressive folding collapse, are higher initially and gradually decrease as shown in Figure 6. Plastic collapse always occurred at one (usually top) end and the deformation front gradually progressed with continued crushing until the plastic folding deformation approached the lower end of the specimen. Then the load increased very rapidly indicating the densification of the specimen.

The single tubes of the honeycomb deformed in diamond mode, adjacent cell walls connected to each other deforming out of phase without any triggering. In axial loading for 80 mm cube specimen, the mean load ( $F_m = 12$  kN) is about 60 times higher compared with simple lateral loading across faces. While the analytical mean load carried out by Wierzbicki (1983) underestimates the experiment by about 20% assuming the flow stress to be equal to the ultimate tensile stress,  $\sigma_{ult}$ . It was found that the average plastic fold,  $\lambda_p (= 2H)$  is 3 mm. A summary of experimental results for aluminium honeycomb under uniaxial compression is presented in Table 1.



(0)  $\delta = 0$  mm



(1)  $\delta = 17$  mm



(2)  $\delta = 34$  mm



(3)  $\delta = 60$  mm

**Figure 5. A sequence of photographs showing the deformation of aluminium honeycomb specimen compressed across corners**

**Conclusions**

The results of aluminium honeycomb subjected to quasi-static compressive loading are studied and presented. The deforming mode in various displacements is observed. The deformation patterns are described and a comparison of the behaviour of honeycomb compressed in different directions is made. It shows that in axial compression, the mean load ( $F_m = 12$  kN) is about 60 times higher compared with simple lateral loading across faces, thus it is shows that the aluminium honeycomb is deformed under uniaxial diamond condition. While the

analytical mean load done by Wierzbicki (1983) underestimates the experiment by about 20%. The collapse load of honeycombs compressed across corners is higher by about 50% compared with loading across faces.

**References**

Reid, S.R. and Peng, C. (1997). Dynamic uniaxial crushing of wood. *Int. J. Impact Eng.*, 19(5-6):531-570.  
 Gibson, L.J. and Ashby, M.F. (1998). *Cellular Solids: Structures and Properties*. 2<sup>nd</sup> ed. Cambridge, UK, University Press, 532p.

**Table 1. A summary of results of aluminium honeycombs under quasi-static compressive loading**

Specimen no. (width x height x length)	Peak load, kN at ( $\delta_p$ , mm)	average $\lambda_p$ at mid foH bacace (mm)	mean Load, $F_m$ (kN)	Energy absorbed, $W$ (J) at up to $\delta = 62$ mm or 50 mm	Mode of deformation	Comment
h3com1	17.4(1.32)	3.0	12	735 (62 mm)	Diamond	80 mm height
h3com2	18.1(0.50)	2.8	12	732 (62 mm)	Diamond	80 mm height
h3com3	16.8(0.80)	2.8	12	745 (62 mm)	Diamond	80 mm height
h3com4	18.8(0.82)	3.0	12	742 (62 mm)	Diamond	80 mm height
h3com-1	38.8(0.60)	3.4	17	838 (50 mm)	Diamond	100 mm height
h3com-2	31.5(0.60)	3.4	17	854 (50 mm)	Diamond	100 mm height

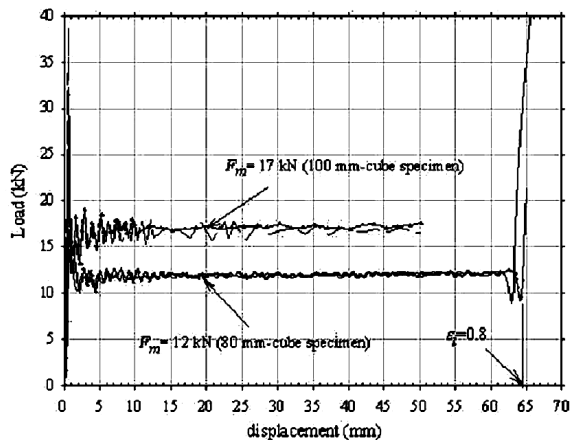


**Figure 6. Load against displacement traces for axially compressed honeycombs showing repeatability. The top traces are for 100 mm-cube and the bottom for 80 mm-cube specimen**

- Reid, S.R., Reddy, T.Y., and Peng, C. (1993). Dynamic compression of cellular structures and materials. In: Structural crashworthiness and Failures. Jones, N. and Wierzbicki, T. (eds.). Elsevier, Amsterdam, p. 295-339.
- Masters, I. and Evans, K. (1996). Models for the elastic deformation of honeycombs, *Composite Structure*, 35:403-422.
- McFarland, R.K. (1963). Hexagonal cell structures under post-buckling axial load. *AIAA J.*, 1(6): 1,380-1,385.
- McFarland, R.K. (1964). The development of metal honeycomb energy absorbing elements. J.P.L. Technical Report, No. 32-639.
- Wierzbicki, T. (1983). Crushing analysis of metal honeycombs. *Int. J. Impact Eng.*, 1(2):157-174.
- Wu, E. and Jiang, W.S. (1997). Axial crush of metallic honeycombs. *Int. J. Impact Eng.*, 19(506):439-456.
- Gibson, L.J., Ashby, M.F., Schajer, G.S., and Robertson, C.I. (1982). The mechanics of two-dimensional cellular materials. *Proceedings of R. Soc., London*, A(382):25-42.
- Klinworth, J.W. and Stronge, W.J. (1988). Elastoplastic yield limits and deformation laws for transversely crushed honeycomb. *Int. J. Mech. Sci.*, 30(314):273-292.
- Klinworth, J.W. and Stronge, W.J. (1989). Plane punch indentation of a ductile honeycomb. *Int. J. Mech. Sci.*, 31:359-378.
- Masters, I.G. and Evan, K.E. (1996). Models for elastic deformation of honeycombs, *Composite Structures*, 35:403-422.
- Triantafyllidis, N. and Schraad, M.W. (1998). Onset of failure in aluminium honeycombs under general in-plane loading. *J. Mech. Phys. Solid.*, 46(6):1,089.
- Papka, S.D. and Kyriakides, S. (1994). In-plane compressive response and crushing of honeycomb. *J. Mech. Phys. Solid.*, 42(10):1,499-1,532.
- Said, M.R and Reddy, T.Y. (2001). The energy absorption of aluminium honeycomb under quasi-static loading. *Proceedings of 4<sup>th</sup> International Conference on Mechanical Engineering*, 2:37-42.